Dyes and Pigments 94 (2012) 81–87

Contents lists available at SciVerse ScienceDirect

Dyes and Pigments

journal homepage: www.elsevier.com/locate/dyepig

Fluorescent nanofibers and microcrystals obtained by reprecipitation of a long-chain iminocoumarin derivative

Hamida Turki [a], Souhir Abid [a], Nathalie Saffon [b], Suzanne Fery-Forgues [c,*]

[a] Laboratory of Applied Chemistry HCGP, Faculty of Science, University of Sfax, 3038 Sfax, Tunisia
[b] Service commun RX, Institut de Chimie de Toulouse, ICT- FR2599, Université Paul Sabatier, 31062 Toulouse Cedex 9, France
[c] Laboratoire des Interactions Moléculaires Réactivité Chimique et Photochimique, CNRS UMR 5623, Université Paul Sabatier, 31062 Toulouse Cedex 9, France

ARTICLE INFO

Article history:
Received 7 October 2011
Received in revised form
26 October 2011
Accepted 27 October 2011
Available online 13 November 2011

Keywords:
Coumarin
Iminocoumarin
Fluorescence
Microcrystal
Nanofiber
Reprecipitation

ABSTRACT

An iminocoumarin derivative bearing a fatty chain, specifically N-palmitoyl-3-cyano-7-diethylamino-2-iminocoumarin, was synthesized and used to prepare particles owing to a solvent exchange process (reprecipitation method). The composition of the reprecipitation medium was allowed to vary. In all cases, very thin particles that emitted yellow–orange light were obtained. In water alone, they looked like nanofibers or nanoribbons. Addition of surfactants at concentrations lower than the CMC favored the formation of bladed microcrystals. In the presence of acetonitrile, elongated microcrystals with good wave-guiding properties were obtained. The fluorescence properties were discussed on the basis of the crystal packing mode. It appears that the flexibility of the imino function leads to an original crystal structure, which is compatible with solid-state fluorescence. This property, together with the ease of synthesis, makes this family of compounds interesting for subsequent use as optically-active nanomaterials.

1. Introduction

In the rapidly expanding field of organic nano- to micrometer-sized materials, fluorescent nanofibers and nanocrystals occupy a very special position. Both of them find potential use in new technology devices [1–7], as well as in the field of chemical and biochemical sensors [8–13]. As a matter of fact, specific applications closely depend on the nature and size of these nano-objects. For instance, the particular shape of nanofibers makes them unique candidates for individual insertion in miniaturized systems where they act as active component to generate or transmit light [6,7]. When they display wave-guiding properties, they can also find original applications such as the authentication of precious documents [7]. In contrast, small round-shaped nanocrystals are particularly useful as fluorescent emitters in living cells for biological studies [14], as well as for medical imaging [15].

The ideal would be that molecules assemble spontaneously to give the desired particles. This would allow easy and cheap preparation of materials using bottom–up approaches. Unfortunately, we miss data to know which chemical modifications must be brought to molecules to favor the formation of a given type of particle. This field has hardly been explored and the task is particularly difficult, since many limitations associated to solid-state fluorescence must simultaneously be taken into account [16,17]. For example, the frequently encountered molecular arrangement where strong head-to-head stacking interactions take place is not compatible with fluorescence emission and must absolutely be avoided.

In this context, our team recently investigated the formation of fluorescent nanoparticles from some coumarin derivatives, using a solvent exchange process called reprecipitation method. Although the studied coumarin derivatives only differed by very small structural changes, an evolution was noted in the shape of the obtained particles. For instance, Coumarin 6 (i.e. 3-(2′-benzothiazolyl)-7-diethylaminocoumarin) and Coumarin 7 (i.e. 3-(2′-benzimidazolyl)-7-diethylaminocoumarin) spontaneously gave microrods [18,19] while the analogs bearing a methyl and a butyl group on the benzimidazolyl group lead to straight and entangled nanofibers, respectively [18]. Obviously, all these molecules show a tendency to give elongated structures, but the formation of nanofibers was unexpected. Actually, the driving force being quite weak, these particles rarely form in a spontaneous way from small molecules, although a few compounds have been reported to give nanofibers via simple solvent-exchange or drop-casting methods

* Corresponding author. Tel.: +33 5 61 55 68 05; fax: +33 5 61 55 81 55.
E-mail address: sff@chimie.ups-tlse.fr (S. Fery-Forgues).

0143-7208/$ – see front matter © 2011 Elsevier Ltd. All rights reserved.
doi:10.1016/j.dyepig.2011.10.018

[11,20–27]. At this stage of the work, increasing significantly the length of the alkyl chain seemed interesting to us. In fact, it is known that the van der Waals interactions that take place between aliphatic groups contribute to stabilize the fibers, together with the π–π interactions due to aromatic groups [6,28]. Unfortunately, long-chain derivatives of Coumarin 7 were tedious to synthesize. Moreover, making a correlation between the spectroscopic behavior and the packing arrangement in the crystal is essential for understanding the emission properties in the solid-state, and our substituted coumarins were quite reluctant to form single crystals of macroscopic size, usable for standard X-ray crystallographic analysis. For these reasons, no further investigation was carried out on this series of dyes and our attention was turned toward closely related structures.

A new work was therefore undertaken in the 3-cyano-7-diethylamino-2-iminocoumarin series. These dyes have been studied by our team for six years [29–33]. Some of them display excellent spectroscopic properties, similar to those of the corresponding coumarins, and their fluorescence behavior can be widely modulated by varying the chemical structure in view of different applications. Another distinct advantage of iminocoumarins is that they lend themselves well to substitution on the imino function, so a large variety of structures can be obtained easily. Moreover, most of these compounds readily crystallize. In the present work, the iminocoumarin derivative **1** (Fig. 1) bearing a fatty chain on the imino function was synthesized and used to prepare particles by the reprecipitation method. The shape and size of the formed particles were studied, as well as the optical properties, which were discussed on the basis of the molecular arrangement obtained by X-ray diffraction analysis.

2. Experimental section

2.1. Materials

Acetone (Carlo Erba) and high-pressure demineralized water (resistivity 18 MΩ cm) prepared with a Milli-Q apparatus (Millipore) were used as solvents. Palmitoyl chloride and Triton TX100 were purchased from Aldrich. Sodium dodecylsulfate and cetyltrimethylammonium bromide were from Acros.

2.2. Preparation of N-palmitoyl-3-cyano-7-diethylamino-2-iminocoumarin (*1*)

Palmitoyl chloride (10 mmol) diluted in 2 mL of chloroform was added dropwise, for 30 min, to a stirred solution of 10 mmol of 3-cyano-7-diethylamino-iminocoumarin [29] in 30 mL of chloroform containing 10 mmol of pyridine, while keeping the mixture at 0 °C. The basic medium was then allowed to reach room temperature and was stirred for 3–4 h. A triple extraction with water was realized. The organic phase was then dried, the solvent was evaporated off and the crude product was precipitated in cyclohexane, filtered and dried. It was purified by TLC chromatography on silica plates using toluene/ethyl acetate 2:1 as the eluent, and extracted with ethylacetate. After solvent evaporation, compound **1** was obtained as a light ochre powder with a yield of 30%. IR (KBr): C≡N (2224 cm^{-1}), C=O (1700 cm^{-1}), C=N (1652 cm^{-1}), C=C (1611 cm^{-1}). ^{1}H NMR (300 MHz, $CDCl_3$): δ ppm = 7.73 (s, 1H, H4), 7.20 (d, J = 9 Hz, 1H, H5), 6.55 (dd, J = 9 Hz, J = 3 Hz, 1H, H6), 6.31 (d, J = 3 Hz, 1H, H8), 3.44 (q, J = 9 Hz, 4H, CH_2–N), 2.57 (t, J = 9 Hz, 2H, CH_2–CO), 1.74 (qn, 9 Hz, 2H, CH_2–CH_2–CO), 1.27 (broad signal, 24H, $(CH_2)_{12}$), 1.23 (q, J = 9 Hz, 6H, CH_3–CH_2–N), 0.90 (t, J = 9 Hz, 3H, CH_3). ^{13}C NMR (75 MHz, $CDCl_3$): δ ppm = 185.91 (C=O), 156.32 (C9), 152.86 (C4), 150.58 (C2), 146.89 (C7), 130.43 (C5), 115.50 (C≡N), 109.27 (C10), 106.55 (C6), 97.17 (C8), 94.82 (C3), 45.25 (CH_2N), 39.07 (CH_2–CO), 31.93 (CH_2–CH_2–CO), 29.70, 29.66, 29.58, 29.46, 29.36, 29.32, 24.53, 22.69 $(CH_2)_{12}$, 14.12 (CH_3–CH_2–N), 12.39 (CH_3). Anal. calc. for $C_{30}H_{45}N_3O_2$: C, 75.11; H, 9.46; N, 8.76. Found: C, 74.89; H, 9.83; N, 8.64 MS: 480 (M + H^+); 497 (M + NH_4^+).

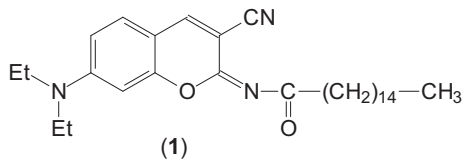

Fig. 1. Chemical structure of the iminocoumarin derivative **1**.

2.3. Crystallographic data for N-palmitoyl-3-cyano-7-diethylamino-2-iminocoumarin (*1*)

Data were collected at low temperature T = 193(2) K on a Bruker-AXS APEX II diffractometer with MoKα radiation (λ = 0.71073 Å) by using phi- and omega-scans. Semi-empirical absorption corrections were employed. The structure was solved by direct methods (SHELXS 97) [34] and all non-hydrogen atoms were refined anisotropically using the least-square method on F^2 [35].

Crystal data for **1**: $C_{30}H_{45}N_3O_2$ M = 479.69, monoclinic, P 2_1/c, a = 23.407(2) Å, b = 13.6876(11) Å, c = 9.0658(7) Å, α = γ = 90°, β = 98.918(5)°, V = 2869.5(4) $Å^3$, Z = 4. In all, 21,215 reflections (4684 independent, R_{int} = 0.1651) were collected. 320 Parameters, 0 restraints, R_1 [$I > 2\sigma(I)$] = 0.0617, $wR2$ [all data] = 0.1879, largest diff. peak and hole: 0.196 and −0.177 e $Å^{-3}$.

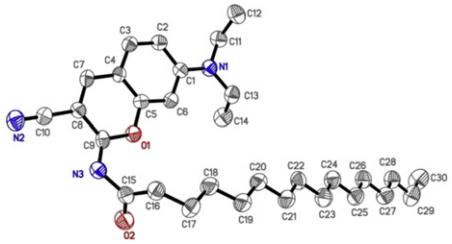

CCDC 854483 contains the supplementary crystallographic data for this structure. These data can be obtained free of charge via www.ccdc.cam.ac.uk/conts/retrieving.html (or for the CCDC, 12 Union Road, Cambridge CB2 1EZ, UK; fax: +441223 336033; e-mail: deposit@ccdc.cam.ac.uk).

2.4. Apparatus

Mass spectra were obtained at the "Service Commun de Spectrométrie de masse de l'Université Paul Sabatier de Toulouse" with a ThermoQuest spectrometer using DCI/NH_3 as the ionization mode. The ^{1}H NMR spectra were recorded on a Bruker AC300 spectrometer operating at 300.13 MHz. The microanalysis was obtained with a Perkin Elmer 2400 series II elemental analyzer in the "Service d'Analyse Chimique du Laboratoire de Chimie de Coordination de Toulouse". Spectroscopic measurements were conducted at 20 °C in a temperature-controlled cell. UV–vis absorption spectra were recorded on a Hewlett–Packard 8452A diode array spectrophotometer. Corrected steady state fluorescence spectra on solutions and suspensions were recorded with a Photon Technology International (PTI) Quanta Master 1 spectrofluorometer. The fluorescence quantum yields (Φ) on solutions and suspensions were determined using the classical formula: $\Phi_x = (A_s \times F_x \times n_x^2 \times \Phi_s)/(A_x \times F_s \times n_s^2)$ where A is the absorbance at the excitation wavelength, F the area under the fluorescence curve

and n the refraction index [36]. Subscripts s and x refer to the standard and to the sample of unknown quantum yield, respectively. Coumarin 6 in ethanol ($\Phi = 0.78$) was taken as the standard [36]. The fluorescence quantum yields were measured by exciting the samples at their absorption maximum. The photoluminescence quantum yield in the solid-state has been measured using a Jobin-Yvon Fluorolog-3 fluorometer equipped with an F-3018 integrating sphere and a UV–vis detector R2658. The sample was mounted as pure solid between two glass cover slips and inserted in the integrating sphere using the solid sample holder. Excitation was performed at 436 and 450 nm. The quantum yield was determined as described elsewhere [37] using the method developed by de Mello et al [38]. The size and shape of the micro/nanoparticles were observed with a Zeiss Axioskop fluorescence microscope equipped with an Andor Luca camera. The excitation wavelength was 430–450 nm, and the emission wavelength was set at around 500–530 nm, using suitable filters. Transmission electron microscopy was performed at the "Service Commun de Microscopie Electronique de l'Université Paul Sabatier", using a JEOL JEM 1011 microscope equipped with a SIS Megaview III camera. To prepare the samples, the carbon grid was soaked into the aqueous suspension containing the iminocoumarin derivative, after reprecipitation was complete. The sample was revealed with a drop of ammonium molybdate (2%, pH 5) as a contrasting agent and allowed to dry for 48 h under vacuum at 60 °C. The X-ray powder diffraction pattern was performed in the "Service Diffraction X du Laboratoire de Chimie de Coordination de Toulouse". It was collected in transmission mode, on capillaries samples, on a θ-θ XPert Pro Panalytical diffractometer, with λ (Cu Kα1, Kα2) 1.54059, 1.54439 Å. The extraction of peak positions for indexing was performed with the fitting program, available in the PC software package Highscore + supplied by Panalytical.

3. Results

3.1. Synthesis and crystal packing mode of the iminocoumarin derivative (*1*)

Compound **1** was obtained by reacting 3-cyano-7-diethylamino-2-iminocoumarin, prepared as previously reported [29] with palmitoyl chloride in the presence of pyridine. The compound was purified and characterized as described in the Experimental Section.

Single crystals of **1** were grown by slow ripening in acetonitrile. An X-Ray diffraction analysis was performed to get insights into the crystal packing mode. Compound **1** crystallizes in the monoclinic system (space group $P\ 2_1/c$). All fatty chains run parallel to each others. The four molecules that constitute the crystal unit are arranged by pairs (for example (a,b) and (c,d) on Fig. 2a), and for each pair the fatty chains are lying some next to the others. Interestingly, the iminocoumarin heterocycles borne by these molecule pairs point toward opposite directions, forming an angle of about 95° between them. Moreover, the heterocycles borne by molecules b and c are superimposed in a head-to-tail fashion. The average plane-to-plane distance is 3.7 Å, indicating significant π–π stacking interactions. The fatty chains were hardly involved in short contacts, contrary to the iminocoumarin moieties. These contacts involve most of the heteroatoms, more specifically the nitrogen atoms of the cyano and imino groups, and the carbonyl oxygen atom (Fig. 2b). They extend the structure into a three-dimensional network (Fig. 2c). Actually, when considering a large number of crystal units, it appears that the crystal is made of layers of fluorophores separated by layers of fatty chains. The distance between two superimposed iminocoumarin heterocycles is 9 Å.

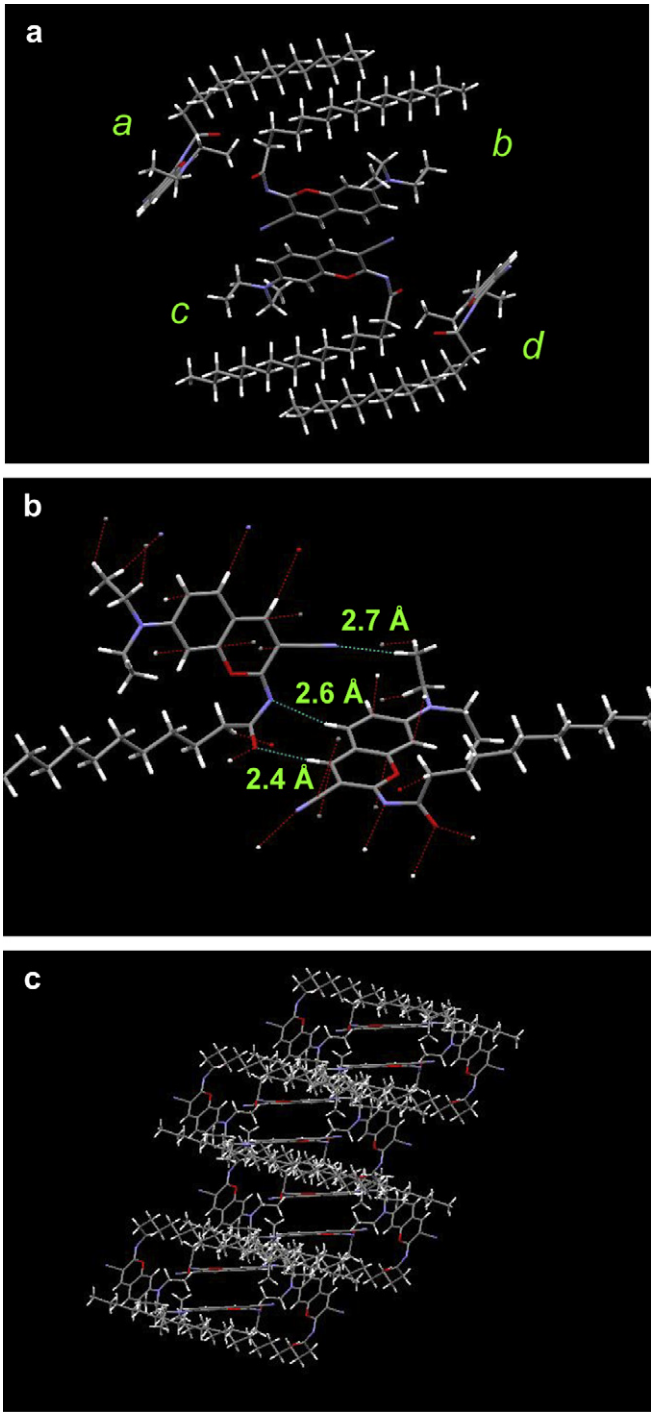

Fig. 2. Crystal packing mode of iminocoumarin derivative **1**. (a) Crystal cell. (b) Short contacts between two neighboring molecules. (c) Overall arrangement.

3.2. Preparation of microparticles

3.2.1. Dye reprecipitation in water

The reprecipitation method [39,40] was used to obtain nano- or microparticles from compound **1**. This simple and mild method, based on a solvent exchange, has been widely developed during the last few years and has proved to be very useful to us in preparing nano and microcrystals of various organic dyes [41–43]. It generally consists in dissolving the organic compound in a hydrophilic solvent, and then pouring a small volume of this concentrated

solution into a large volume of water. The organic compound then precipitates, thus leading to the formation of nano- or microparticles in aqueous suspension. In the present case, a stock solution of compound **1** (1×10^{-2} M) in acetone was prepared and an aliquot (40 μL) of this solution was injected into a cell containing 1.96 mL of water. The final dye concentration was therefore 2×10^{-4} M and the proportion of acetone in water was 2%. The sample turned slightly cloudy after introducing the dye solution into water. The mixture was then left under stirring at room temperature.

Two hours after the beginning of the reprecipitation process, a drop of the suspension was placed between two glass slides and observed with a fluorescence microscope. The sample exhibited a large number of elongated particles that showed a tendency to agglomeration and emitted yellow–orange fluorescence (Fig. 3a). Interestingly, the fluorescence did not fade upon irradiation by the microscope light beam. The sample was also analyzed by transmission electron microscopy (TEM). To do so, a drop of suspension was deposited on a grid, dried and stained by a contrasting agent. The sample showed the same type of particles, which resembled nanofibers or nanoribbons (Fig. 3b). The size was heterogeneous. The biggest particles had a length of about 4 μm and a width of 200 nm, their thickness was estimated to be between 90 and 130 nm. Side-by-side agglomeration gives the impression of biggest particles.

These thin particles did not give any electron diffraction spectrum. To get more information about their possible crystallinity, a large volume of suspension was prepared in the same experimental conditions as above. This suspension was filtered on a Nylon membrane filter (0.45 μm) and the solid residue was dried under vacuum. An X-ray powder diffraction pattern was recorded, confirming the crystalline nature of the filtered material. The comparison of this experimental pattern with the one calculated from X-Ray analysis shows many similarities, indicating that the crystal packing mode has been retained after reprecipitation, although some amorphization occured (Fig. 4).

3.2.2. Dye reprecipitation in the presence of additives

In some of our previous works [41–43], the presence of additives in the reprecipitation medium allowed the size and shape of the microcrystals obtained to be markedly modified. Surfactants and polymers have also been used in the literature to govern the formation of nanofibers [22,26,27]. In the present work, the effect of three surfactants on the reprecipitation of **1** was investigated. Sodium dodecyl sulfate (SDS), cetyltrimethylammonium bromide (CTAB) and Triton TX100 were chosen as anionic, cationic and neutral surfactants, respectively. They were used at the concentration of 6×10^{-3} M, 8×10^{-4} M, and 1×10^{-4} M, respectively, that is below the critical micelle concentration (CMC), in order to avoid dye solubilization into the micelles. The additives were dissolved in water prior to mixing with the dye acetone solution and reprecipitation experiments were run as described above, the final dye concentration being 2×10^{-4} M. The samples were observed 2 h after the beginning of the reprecipitation process.

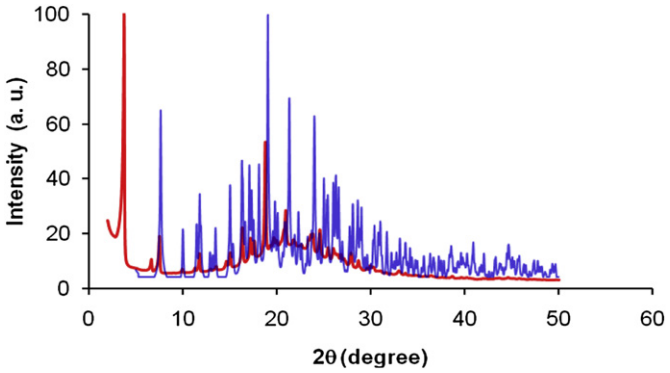

Fig. 4. Red line: Experimental XRPD pattern recorded after reprecipitation of **1** in water. Blue line: Pattern calculated from the X-ray data of **1**, recorded on a single crystal. (For interpretation of the references to color in this figure legend, the reader is referred to the web version of this article.)

With the fluorescence microscope, none of the samples showed agglomerates of elongated particles similar to those obtained in water alone. However, they all contained flat particles that emitted yellow–orange light. The light emitted by the edges was particularly strong. Their geometrical shape evoked very thin, bladed microcrystals. Some of them were twinned. In the presence of CTAB, the formed structures were regular, rectangular plates. Their average size was about 6–10 μm × 1.5 μm, their maximum size being 25 μm × 5 μm (Fig. 5a). With SDS and Triton, the average crystals were small (around 2 μm long) and of irregular shape, like torn, although big particles were sometimes noticed (Fig. 5b). The observation by TEM confirmed the presence of very flat and thin particles in the three samples. Two examples are given in Fig. 6. All the particles emitted an electron diffraction spectrum that vanished almost instantly, indicating their crystalline nature.

3.2.3. Dye reprecipitation in the presence of acetonitrile

Reprecipitation was also carried out according to another procedure. An aliquot (40 μL) of the concentrated acetone solution of **1** was mixed with 0.6 mL acetonitrile, and then 1.36 mL water was added. The final dye concentration was 2×10^{-4} M. In this case, elongated microcrystals with a rectangular shape, measuring up to 30 μm, were observed (Fig. 7). Some of them were twin crystals. Their tips were intensely bright, while their bodies exhibited relatively weaker emission.

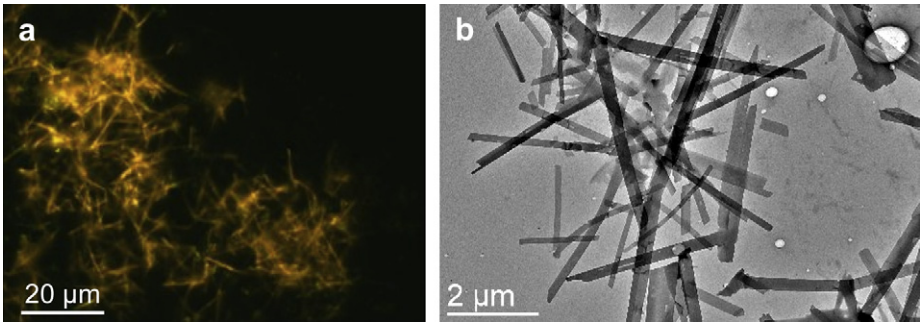

Fig. 3. Fluorescence microscopy image (a) and transmission microscopy image (b) of aqueous suspensions of **1** (2×10^{-4} M) after reprecipitation in water with 2% v/v acetone.

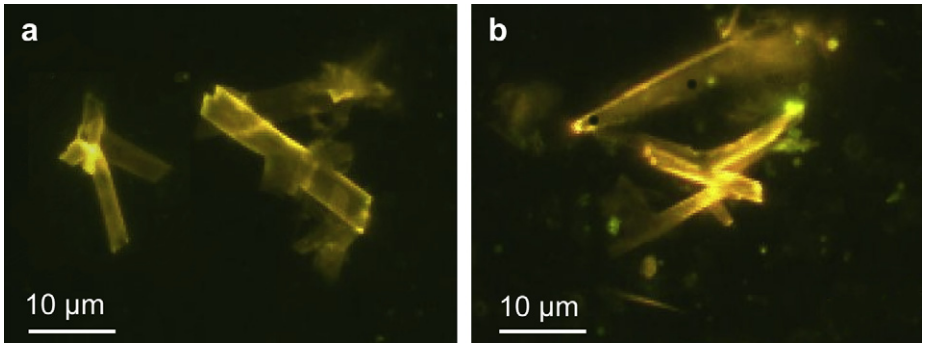

Fig. 5. Fluorescence microscopy image of aqueous suspensions of **1** (2×10^{-4} M) after reprecipitation in water with 2% v/v acetone in the presence of (a) CTAB (8×10^{-4} M) and (b) TX100 (1×10^{-4} M).

3.3. Spectroscopic study

Before studying the behavior of **1** in the solid-state, a cursory glance was given at the spectroscopic properties of this dye dissolved in six organic solvents of various polarities (Table 1). The absorption and fluorescence excitation spectra were very similar and both displayed an intense band that was red-shifted with increasing polarity. The emission spectra showed one intense unresolved band, the maximum of which was shifted to the red by 42 nm when passing from toluene to ethanol (Fig. 8). This behavior is in total agreement with that reported for other iminocoumarin derivatives [30,31,33] and more precisely for the analog of **1** that bears an acetyl group instead of the palmitoyl group [33]. Positive solvatochromism is a characteristic of this series of compounds, which undergo strong enhancement of the dipole moment in the excited state. The fluorescence quantum yield was high in apolar solvents, and was markedly decreased with increasing polarity. This phenomenon can be attributed to the stabilization of a non-emissive twisted internal charge transfer (TICT) state by polar solvents, as reported for 7-alkylaminocoumarins [44–46].

The solid-state photoluminescence properties were investigated on the microcrystalline powder directly issued from synthesis. An integration sphere was used to avoid the many drawbacks linked to the spectroscopy of highly absorbing media. Microcrystals of **1** exhibited photoluminescence, with an unresolved single band centered on 535 nm. The solid species therefore emits at much longer wavelength than the dissolved molecules (Fig. 8). The photoluminescence quantum yield was quite low, only 0.042 ± 0.002.

4. Discussion

It was shown in our previous works that Coumarins 6 and 7 give rod-like microcrystals by the reprecipitation method [18,19]. The substitution of the benzimidazolyl nitrogen atom of Coumarin 7 by a short aliphatic chain enhances this tendency and leads to the spontaneous formation of nanofibers, which actually result from an elongation of the crystal. The present study shows that, like coumarins, the iminocoumarin derivative **1** gives elongated nano/microstructures by reprecipitation. Particles resembling nanofibers were obtained in water. But, they cannot be compared to those made of molecules that bear both a large aromatic moiety and a bulky aliphatic moiety, as reported in the literature [6]. In this case, the aromatic rings are generally lying some on the others, and the aliphatic groups are involved in van der Waals interactions. These various interactions stabilize a one-dimension molecular arrangement, often leading to more complex, hierarchical organizations [47,48]. This type of arrangement was not observed here, maybe because the aromatic moiety is too small to induce strong stacking effect, or because the alkyl moiety is not large enough.

Grafting a fatty chain of moderate length on the imino function is therefore not enough for modifying totally the molecular organization. This probably also explains why crystallization is not prevented, as it usually happens for compounds that bear long alkyl chain. Actually, the iminocoumarin derivative **1** crystallizes readily in various experimental conditions. However, the palmitoyl moiety strongly influences the characteristics and behavior of compound **1** in the solid-state. In the crystal, the fatty chains form a distinct layer where they run parallel to each other, and therefore induce the appearance of an original packing mode. Particularly interesting is also the fact that the shape and size of the obtained nano/microparticles depend on the presence of additives. In water alone, thin and elongated particles were obtained. In the presence of surfactants, and in particular CTAB, the particles widen and so compound **1** gives large microcrystals with a nanometric dimension. All these particles can be seen as a modification of the crystal. A comparable sensitivity to the reprecipitation conditions was already encountered in the course of our studies of a nitrobenzoxadiazole (NBD) derivative provided with an *n*-octyl chain. With this compound,

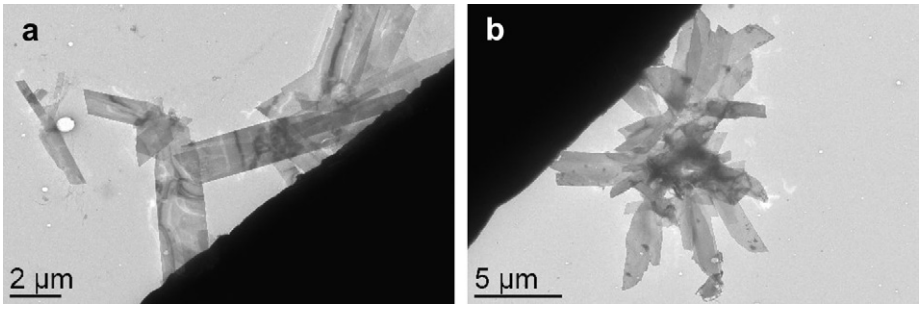

Fig. 6. Transmission microscopy image of aqueous suspensions of **1** (2×10^{-4} M) after reprecipitation in water with 2% v/v acetone in the presence of additives: (a) CTAB (8×10^{-4} M); (b) SDS (6×10^{-3} M).

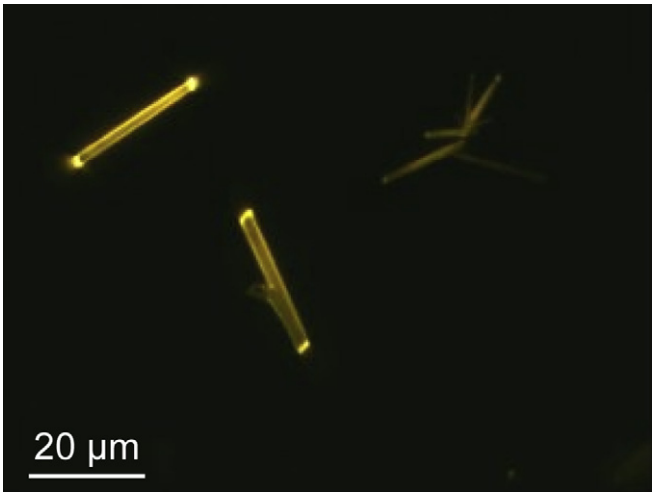

Fig. 7. Fluorescence microscopy image of aqueous suspensions of **1** after reprecipitation in water with 30% v/v acetonitrile and 2% v/v acetone. Dye concentration: (2×10^{-4} M).

spectacular variations of the shape and size of the obtained microcrystals were observed, according to the nature of the additive (polymers or surfactants below the CMC) placed in the reprecipitation medium [41–43]. These variations were attributed to the selective adsorption of the additive molecules on the crystal faces, some of which are highly hydrophobic [49] and subsequent interactions with crystal growth without variation in the crystal packing mode. This behavior was not observed with Coumarin 7 and its derivatives that bear a small alkyl group. It could be interesting to check on other molecules if the association of a small aromatic moiety with a fatty chain bestows the compound a particular sensitivity to the presence of additives in the reprecipitation medium.

All the nano/microparticles obtained by reprecipitation of **1** are fluorescent. To understand the origin of this fluorescence, let us consider the crystal packing mode. It can be seen that the molecules are organized by pairs, the fatty chains running parallel to each others to maximize the van der Waals interactions. The risk, with such an arrangement, is that the aromatic heterocycles borne by the fatty chains are superimposed, this side-by-side stacking being highly disadvantageous for fluorescence [16,17]. However, in the present case, the fluorophores belonging to the same pair are displayed perpendicularly, and so the transition dipole moments have little interaction between them [50,51]. Moreover, each fluorophore is arranged head-to-tail with respect to its closest neighbor, therefore entailing an additional stabilization of the transition moments [16,17,50,51]. This conformation is allowed by the flexibility of the imido group and it is rigidified by the numerous interactions that involve the heteroatoms borne by the cyano and imino groups. The formation of layers also prevents interactions between superimposable fluorophores. This arrangement is reminiscent of that recently encountered in the course of

Table 1
Maximum absorption (λ_{abs}) and emission (λ_{em}) wavelengths, and fluorescence quantum yields (Φ) of compound **1** in different media. Excitation at λ_{abs}.

	λ_{abs}	λ_{em}	Φ
Toluene	420	474	0.61 ± 0.01
Ethyl acetate	420	488	0.66 ± 0.01
Tetrahydrofuran	422	490	0.72 ± 0.01
Acetone	428	496	0.25 ± 0.01
Ethanol	430	516	0.16 ± 0.01
Dimethylsulfoxide	430	504	0.11 ± 0.01

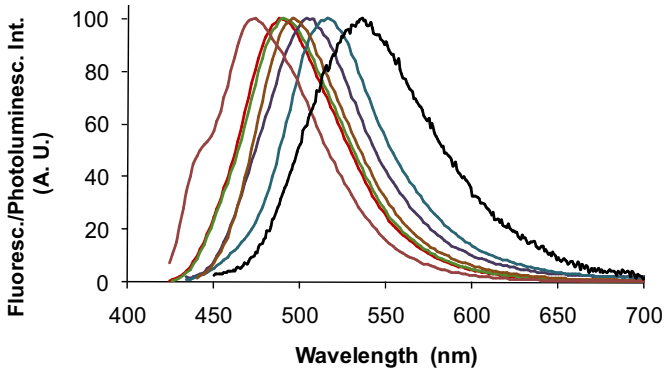

Fig. 8. From left to right: Normalized fluorescence emission spectra of compound **1** in various organic solvents (toluene, ethyl acetate, tetrahydrofuran, acetone, dimethylsulfoxide, ethanol, respectively) with excitation at the maximum absorption wavelength; photoluminescence emission spectrum (λ_{ex} = 436 nm) of the microcrystalline powder of **1**.

our studies about fluorescent ion pairs, where a fluorescent aromatic ion was associated to a bulky aliphatic counter-ion [52,53]. As a consequence, the whole molecular arrangement should be favorable to fluorescence. However, the photoluminescence quantum yield of microcrystalline **1** is not very high. It is one order of magnitude lower than in organic solvent solutions. A better value could have been expected on the basis of the molecular arrangement. An explanation is that fluorescence is deactivated through the numerous short contacts that take place between molecules. Another possibility is that it is affected by the presence of impurities and surface defects. Some positive points must also be underlined. For instance, the reprecipitation of **1** in the presence of acetonitrile leads to the formation of regular rod-like microcrystals that clearly display a phenomenon of wave-guiding [20–22,54] and could find applications as individual optical components. Moreover, the photostability of the particles is of particular interest.

5. Conclusion

The iminocoumarin derivative studied in this work leads to nano and microcrystals using the simplest conditions of the reprecipitation method. The size and shape of the obtained particles strongly depend on the experimental conditions. The flexibility of the imino function and the interactions due to the various heteroatoms lead to an original crystal structure, which is compatible with fluorescence in the solid-state. Owing to its ease of synthesis, this family of iminocoumarin derivatives is therefore promising for the preparation of solid-state emissive compounds. Work is presently underway to prepare new iminocoumarin derivatives in order to study the structure/properties relationship, regarding the formation of nanoparticles and their spectroscopic properties. Special attention will be brought to improving photoluminescence efficiency, for example by bringing steric constraints and incorporating bulky groups to limit short contacts between molecules. Our hope is that these compounds could be useful as optically-active nanomaterials.

Acknowledgments

The authors acknowledge the French Ministry of Foreign and European Affairs and the Ministry of Higher Education, Scientific Research and Technology in Tunisia for their financial support (PHC-Utique program, managed by CMCU, action intégrée n° 11G 1204). We would also like to thank Mr Laurent Weingarten (Service Commun de Microscopie Electronique de l'Université Paul Sabatier,

Toulouse) for TEM measurements, Dr Laure Vendier (Service Diffraction X du Laboratoire de Chimie de Coordination de Toulouse) for the powder X-ray diffraction patterns, and Dr Martine Cantuel (CNRS post-doctoral fellowship, Université de Bordeaux 1) for the measurement of the photoluminescence quantum yield.

References

[1] Lim SJ, An BK, Jung SD, Chung MA, Park SY. Angewandte Chemie International Edition 2004;43:6346–50.
[2] Quian G, Dai B, Luo M, Yu D, Zhan J, Zhang Z, et al. Chemistry of Materials 2008;20:6208–16.
[3] Botzung-Appert E, Zaccaro J, Gourgon C, Usson Y, Baldeck PL, Ibanez A. Journal of Crystal Growth 2005;283:444–9.
[4] Brewer J, Schiek M, Luetzen A, Al Shamery K, Rubahn HG. Nano Letters 2006; 6:2656–9.
[5] Ner Y, Grote JG, Stuart JA, Sotzing GA. Angewandte Chemie International Edition 2009;48:5134–8.
[6] Fery-Forgues S, Fournier-Noël C. Organic fluorescent nanofibers and submicrometer rods. In: Kumar A, editor. Nanofibers. In-Techweb. Available on the Internet: http://www.sciyo.com/books/show/title/nanofibers; 2010.
[7] Schiek M, Balzer F, Al-Shamery K, Brewer JR, Lützen A, Rubahn HG. Small 2008;4:176–81. and refs. cited.
[8] Zhou Y, Bian G, Wang L, Dong L, Wang L, Kan J. Spectrochimica Acta Part A 2005;61:1841–5.
[9] Jinshui L, Lun W, Feng G, Yongxing L, Yun W. Analytical and Bioanalytical Chemistry 2003;377:346–9.
[10] Monnier V, Dubuisson E, Sanz-Menez N, Boury B, Rouessac V, Ayral A. Microporous and Mesoporous Materials 2010;132:531–7.
[11] Che Y, Zang L. Chemical Communications 2009;34:5106–8.
[12] Law B, Weissleder R, Tung CH. Bioconjugate Chemistry 2007;18:1701–4.
[13] Tao S, Li G, Yin JJ. Mater. Chem. 2007;17:2730–6.
[14] Yu Y, Feng C, Hong Y, Liu J, Chen S, Ng KM, et al. Advanced Materials 2011;23: 3298–302.
[15] Parthasarathy V, Fery-Forgues S, Campioli E, Recher G, Terenziani F, Blanchard-Desce M. Small 2011;7:3219–29.
[16] Birks JB. Photophysics of aromatic molecules. London: Wiley; 1970.
[17] Krasovitskii BM, Bolotin BM. Organic luminescent materials. Weinheim, Germany: VCH; 2002.
[18] Mille M, Lamère JF, Rodrigues F, Fery-Forgues S. Langmuir 2008;24:2671–9.
[19] Fery-Forgues S, El-Ayoubi R, Lamère JF. Journal of Fluorescence 2008;18: 619–24.
[20] Zhao YS, Xu J, Peng A, Fu H, Ma Y, Jiang L, et al. Angewandte Chemie International Edition 2008;47:7301–5.
[21] Zhao YS, Peng A, Fu H, Ma Y, Yao J. Advanced Materials 2008;20:1661–5.
[22] Yu H, Qi L. Langmuir 2009;25:6781–6.
[23] An BK, Lee DS, Lee JS, Park YS, Song HS, Park SY. Journal of the American Chemical Society 2004;126:10232–3.
[24] An BK, Gihm SH, Chung JW, Park CR, Kwon SK, Park SY. Journal of the American Chemical Society 2009;131:3950–7.
[25] Li S, He L, Xiong F, Li Y, Yang G. Journal of Physical Chemistry B 2004;108: 10887–92.
[26] Fu H, Xiao D, Yao J, Yang G. Angewandte Chemie International Edition 2003; 42:2883–6.
[27] Zhang XJ, Zhang XH, Shi WS, Meng XM, Lee C, Lee ST. Journal of Physical Chemistry B 2005;109:18777–80.
[28] Hoeben FJM, Jonkheijm P, Meijer EW, Schenning APHJ. Chemical Reviews 2005;105:1491–546.
[29] Turki H, Abid S, Le Bigot Y, Fery-Forgues S, El Gharbi R. Synthetic Communications 2004;34:3553–63.
[30] Turki H, Abid S, El Gharbi R, Fery-Forgues S. Comptes Rendus Chimie 2006;9: 1252–9.
[31] Turki H, Abid S, Fery-Forgues S, El Gharbi R. Dyes and Pigments 2007;73: 311–6.
[32] Fakhfakh M, Turki H, Abid S, El Gharbi R, Fery-Forgues S. Journal of Photochemistry and Photobiology A 2007;185:13–8.
[33] Fakhfakh M, Turki H, Fery-Forgues S, El Gharbi R. Dyes and Pigments 2010;84: 108–13.
[34] Sheldrick GM. Acta Crystallographica A 1990;46:467–73.
[35] Sheldrick GM. Acta Crystallographica, Section A 2008;64:112–22.
[36] Reynolds GA, Drexhage KH. Optics Communications 1975;13:222–5.
[37] Fery-Forgues S, Cantuel M, Fournier-Noël C. Dyes and Pigments 2010;87: 241–8.
[38] De Mello JC, Wittmann HF, Friend RH. Advanced Materials 1997;9:230–2.
[39] Nakanishi H, Oikawa H. In: Masuhara H, Nakanishi H, Sasaki K, editors. Single organic nanoparticles. Berlin: Springer-Verlag; 2003. p. 17–31 [Chapter 2].
[40] Kasai H, Nalwa HS, Oikawa H, Okada S, Matsuda H, Minami N, et al. Japanese Journal of Applied Physics 1992;31:L1132–4.
[41] Bertorelle F, Lavabre D, Fery-Forgues S. Journal of the American Chemical Society 2003;125:6244–53.
[42] Bîrlă L, Bertorelle F, Rodrigues F, Badré S, Pansu R, Fery-Forgues S. Langmuir 2006;22:6256–65.
[43] Abyan M, De Caro D, Fery-Forgues S. Langmuir 2009;25:1651–8.
[44] Jones II G, Jackson WR, Choi CY, Bergmark WR. Journal of Physical Chemistry 1985;89:294–300.
[45] López Arbeloa T, López Arbeloa F, Tapia MJ, López Arbeloa I. Journal of Physical Chemistry 1993;63:203–14.
[46] Wagner BD. Molecules 2009;14:210–37.
[47] Würthner F, Yao S, Beginn U. Angewandte Chemie International Edition 2003; 42:3247–50.
[48] Qu S, Zhao L, Yu Z, Xiu Z, Zhao C, Zhang P, et al. Langmuir 2009;25:1713–7.
[49] Pèpe G, Fery-Forgues S, Jouanna P. Journal of Crystal Growth 2011;333:25–35.
[50] Cornil J, Beljonne D, Dos Santos DA, Calbert JP, Shuai Z, Brédas JL. Comptes Rendus de l'Académie des Sciences Paris, Series IV; 2000:403–8.
[51] Xie Z, Yang B, Li F, Cheng G, Liu L, Yang G, et al. Journal of the American Chemical Society 2005;127:14152–3.
[52] Lamère JF, Saffon N, Dos Santos I, Fery-Forgues S. Langmuir 2010;26:10210–7.
[53] Chahine J, Saffon N, Cantuel M, Fery-Forgues S. Langmuir 2011;27:2844–53.
[54] Takazawa K. Journal of Physical Chemistry C 2007;111:8671–6.